Analytical Biochemistry 380 (2008) 174–183

Contents lists available at ScienceDirect

Analytical Biochemistry

journal homepage: www.elsevier.com/locate/yabio

Zinc oxide/redox mediator composite films-based sensor for electrochemical detection of important biomolecules

Chun-Fang Tang, S. Ashok Kumar, Shen-Ming Chen *

Department of Chemical Engineering and Biotechnology, National Taipei University of Technology, No 1, sec 3,Chung-Hsiao East Road, Taipei 106, Taiwan, Republic of China

ARTICLE INFO

Article history:
Received 2 January 2008
Available online 7 June 2008

Keywords:
Zinc oxide
Core/Shell
Serotonin
Modified electrodes
Electrocatalysis of dopamine
Ascorbic acid
Uric acid

ABSTRACT

Electrochemical oxidation of serotonin (SN) onto zinc oxide (ZnO)-coated glassy carbon electrode (GCE) results in the generation of redox mediators (RMs) that are strongly adsorbed on electrode surface. The electrochemical properties of zinc oxide-electrogenerated redox mediator (ZnO/RM) (inorganic/organic) hybrid film-coated electrode has been studied using cyclic voltammetry (CV). The scanning electron microscope (SEM), atomic force microscope (AFM), and electrochemical techniques proved the immobilization of ZnO/RM core/shell microparticles on the electrode surface. The GCE modified with ZnO/RM hybrid film showed two reversible redox peaks in acidic solution, and the redox peaks were found to be pH dependent with slopes of −62 and −60 mV/pH, which are very close to the Nernst behavior. The GCE/ZnO/RM-modified electrode exhibited excellent electrocatalytic activity toward the oxidations of ascorbic acid (AA), dopamine (DA), and uric acid (UA) in 0.1 M phosphate buffer solution (PBS, pH 7.0). Indeed, ZnO/RM-coated GCE separated the anodic oxidation waves of DA, AA, and UA with well-defined peak separations in their mixture solution. Consequently, the GCE/ZnO/RMs were used for simultaneous detection of DA, AA, and UA in their mixture solution. Using CV, calibration curves for DA, AA, and UA were obtained over the range of 6.0×10^{-6} to 9.6×10^{-4} M, 1.5×10^{-5} to 2.4×10^{-4} M, and 5.0×10^{-5} to 8×10^{-4} M with correlation coefficients of 0.992, 0.991, and 0.989, respectively. Moreover, ZnO/RM-modified GCE had good stability and antifouling properties.

Zinc oxide (ZnO)[1] plays an important role in a wide range of applications because it is an *n*-type semiconductor with wide band gap energy of 3.3 eV and it shows superior optical transparency in the visible region. Furthermore, nontoxic ZnO has good environmental acceptability, is inexpensive, has biocompatibility material, and is plentiful. ZnO is an important optoelectronic material and has been used in a wide range of applications such as solar cells, piezoelectric element, pharmaceuticals, paints, ceramics, surface acoustic wave element, and sensors [1–11]. Alternatively, conjugate polymers have been combined with *n*-type inorganic semiconductor nanoparticles, and such hybrid polymer/inorganic nanocomposite materials may combine the advantages of polymer semiconductors and high electron mobility of inorganic semiconductors [12–14].

Dopamine (DA) is an important neurotransmitter molecule of catecholamines that is widely distributed in the mammalian central nervous system for message transfer. Hence, it has been of interest to neuroscientists and chemists. Loss of DA-containing neurons may result in some serious diseases such as Parkinsonism [15–18]. Therefore, determination of the concentration of this neurochemical is an important task. The fact that DA and other catecholamines are easily oxidizable compounds makes their detection possible by electrochemical methods. A major problem of electrochemical detection of DA in real biological matrices is the coexistence of many interfering compounds. Among these, ascorbic acid (AA) is of particular importance. For example, in the extracellular fluid of the central nervous system, this species is present in very high concentrations (100–500 μM) [19,20]. Uric acid (UA) is the primary end product of purine metabolism. Abnormal levels of UA are symptoms of several diseases such as hyperuricemia, gout, and Lesch–Nyan disease [21]. Other diseases, such as leukemia and pneumonia, are also associated with enhanced urate levels [22]. Moreover, at nearly all bare electrodes, DA, AA, and UA get oxidized at nearly the same potential, resulting in overlapped voltammetric response.

To overcome the above obstacles, the development of modified electrodes for the detection AA, DA, and UA are reported by modifying bare glassy carbon electrode (GCE), platinum, and gold electrodes [20,23,24]. During recent years, substantial efforts have been devoted to the development of electrochemical sensors based on electrodes modified by electrosynthesized polymeric

* Corresponding author. Fax: +886227025238.
E-mail address: smchen78@ms15.hinet.net (S.-M. Chen).

[1] *Abbreviations used:* ZnO, zinc oxide; DA, dopamine; AA, ascorbic acid; UA, uric acid; GCE, glassy carbon electrode; PGE, pyrolytic graphite electrode; SN, serotonin; RM, redox mediator; SEM, scanning electron microscope; AFM, atomic force microscope; ITO, indium tin oxide; TAD, tryptamine-4,5-dione; DHT, 4,5-dihydroxytryptamine; PBS, phosphate-buffered saline; CV, cyclic voltammetry; DOQ, dopamine-*o*-quinone; LOD, limit of detection; RSD, relative standard deviation.

0003-2697/$ - see front matter © 2008 Elsevier Inc. All rights reserved.
doi:10.1016/j.ab.2008.06.004

films. Polymeric films of 3-methylthiophene, aniline, and pyrrole are reported as being useful in the selective detection of DA in excess of AA [25,26]. Poly(cresol red)-modified electrodes [27] and poly(bromophenol blue)-modified electrodes [28] are used to detect AA and DA. It has been reported that electrode covalently modified with poly(vinyl alcohol) [23] and poly(chromotrope 2B)-modified electrodes [29] are useful for simultaneous determination of AA, DA, and UA. Ruthenium oxide-modified electrode could attain simultaneous determination of AA and DA in the presence of UA [30]. Recently, poly(4-amino-1-1′-azobenzene-3,4′-disulfonic acid)-coated electrode for selective detection of DA in the presence of UA, AA, and NADH [31], poly(eriochrome black T)-modified GCE [32], poly(acrylic acid)-multiwalled carbon nanotube composite-covered GCE [33], PtAu hybrid film-modified electrode [34], pyrolytic graphite electrode (PGE) modified into DA solution [35], and carbon ceramic electrode prepared by sol–gel technique [36] have been reported for simultaneous determination of AA, DA, and UA.

In this article, we report for the first time the electrochemical oxidation of serotonin (SN) on ZnO-coated electrode. Surface characterizations and electrochemical properties were studied. It was found that GCE/ZnO/redox mediator (RM)-coated electrode has excellent electrocatalytic properties toward AA, DA, and UA in neutral buffer solution. Here ZnO/RM hybrid film-coated electrode was successfully employed for simultaneous determination of DA, AA, and UA in their mixture solution.

Materials and methods

All chemicals and reagents used in this work were of analytical grade and used as received without further purification. 3-(2-Aminoethyl)-5-hydroxyindole hydrochloride, dopamine hydrochloride (purity 98%), and UA (purity 99%) were purchased from Sigma–Aldrich (St. Louis, MO, USA). Sulfuric acid (purity 95%) and sodium hydroxide (purity 93%) were purchased from Wako Pure Chemicals (Osaka, Japan). AA (purity 99%), sodium acetate, potassium nitrate, zinc nitrate, and sodium dihydrogen phosphate were obtained from E-Merck (Darmstadt, Germany). The aqueous solutions were prepared by using doubly distilled deionized water, and before each experiment the solutions were deoxygenated by purging with prepurified nitrogen gas.

Electrochemical measurements were performed with a CH Instruments (Austin, TX, USA) model 400 potentiostat with conventional three-electrode cell. A BAS glassy carbon and platinum wire were used as the working electrode and auxiliary electrode, respectively. All of the cell potentials were measured with respect to an Ag/AgCl [KCl (sat)] reference electrode. Amperometric studies were performed with a bi-potentiostat model CHI750A (CH Instruments) having an analytical rotator model AFMSRK with MSRX speed control (Pine Instruments, USA). A Hitachi Scientific Instruments (London, UK) model S-3000H scanning electron microscope (SEM) was used for surface image measurements. The atomic force microscope (AFM) images were recorded with a multimode scanning probe microscope system operated in tapping mode using a model CSPM4000 instrument (Ben Yuan, Beijing, China). Vitamin C tablets (500 mg) and dopamine hydrochloride injection were purchased from a local drug store in Taipei, Taiwan. All experiments were carried out at room temperature.

Modified electrode preparation

Prior to the electrode modification, the GCE was mechanically polished with alumina powder (Al_2O_3, 0.05 μm) to a mirror finish and ultrasonicated in distilled water for 5 min. Then GCE was electrochemically activated by using 10 times cyclic potential sweeps in the range of −0.5 to 2.0 V in 0.1 M nitric acid solution at a scan rate of 50 mV s^{-1}. Indium tin oxide (ITO)-coated glass substrates were cleaned by using detergent (Palmolive dishwashing liquid and antibacterial hand soap) and diluted hydrochloric acid and then finally were rinsed with distilled water.

ZnO films were deposited onto GCE or ITO electrode from the bath solution containing 0.1 M KNO_3 and 0.1 M $Zn(NO_3)_2$, as reported previously [37–39]. The electroprecipitation of ZnO thin films from nitrate bath was followed by the following reactions:

$$NO_3^- + H_2O + 2e^- \rightarrow 2NO_2^- + 2OH^- \quad (1)$$

$$Zn^{2+} + 2OH^- \rightarrow Zn(OH)_2 \rightarrow ZnO + H_2O \quad (2)$$

$$Zn^{2+} + NO_3^- + 2e^- \rightarrow ZnO + NO_2^- \quad (3)$$

For the preparation of ZnO/RM composite-modified electrode, the GCE/ZnO electrode was cycled in 0.5 mM SN monomer solution under the same conditions as in the electrode activation procedure. The as-prepared light blue-colored films were smooth and strongly adherent to the electrode substrates. Subsequently, the modified electrode was rinsed thoroughly with distilled water and then dried in air for 30 min at room temperature. For comparison, GCE/ZnO and GCE/RM electrodes were prepared to investigate their electrochemical properties toward the analytes under investigation.

Results and discussion

Electrochemical preparation of ZnO/RM hybrid film-coated electrode and its electrochemical properties

Fig. 1 depicts the electrochemical oxidation of SN onto GCE/ZnO-modified electrode. As can be seen in cyclic voltammograms, on the first anodic scan, irreversible oxidation peak (P_{a1}) was observed at a peak potential of approximately 0.65 V due to the oxidation of SN monomers [40]. On scan reversal, a cathodic wave (P_{C1}) centered at −0.12 V was observed. On the second and subsequent potential scans, two additional anodic peaks (P_{a2} = +0.19 V and P_{a3} = +1.2 V) and a new cathodic peak (P_{C2} = 0.15 V) were observed. After the fifth cycle, in addition to P_{a3}, a broad current shoulder at a potential of +1.60 V appeared. This type of observation was previously reported for polyazine by Ivanova and Karyakin [41], who suggested that a permanent increase in the current of monomer irreversible oxidation indicates both the catalytic

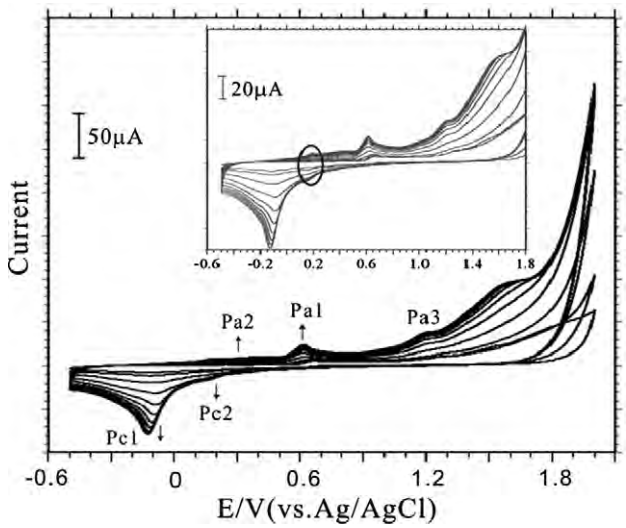

Fig. 1. Electrochemical oxidation of SN onto ZnO-coated GCE from the electrolyte 0.1 M HNO_3 solution containing 0.5 mM SN monomers. Scan rate = 50 mV/s. The inset shows the magnification image of RM film growth.

properties of the resulting electrode coverage and its electronic conductivity. This significant improvement of monomer oxidation in the course of film growth is the property of highly conductive polymers such as polypyrrole and polyaniline.

Then larger peaks were observed in Fig. 1 on continuous scanning, reflecting the continuous adsorption of the oxidation products on the electrode surface. The inset of Fig. 1 shows the high magnification image of RM film growth onto the electrode surface. These facts indicated that RMs were deposited onto the surface of ZnO-modified GCE by electrooxidation. Thereafter, RM-modified GCE was thoroughly washed with doubly distilled water and dried in air for 30 min. Uniform adherent light blue color films were seen on the surface of ZnO-modified GCE. Electrochemical oxidation of SN at 2.0 V in acidic solution results in the generation of the RM 5,5′-dihydroxy-4,4′-bitryptamine on the ZnO films. Initially, a reactive carbocation is formed and either undergoes nucleophilic attack by water or reacts with SN-forming dimers and trimers [40]. The electrogenerated products have a redox-active quinone–imine structure [40,42,43]. Wrona and Dryhurst reported that all oxidation products of SN are cationic and soluble in phosphate buffer and have a high affinity for adsorption on carbon electrode [40]. However, visible accumulation of insoluble light blue color films on the electrode surface strongly indicated that RMs were adsorbed in this case.

Fig. 2 shows the cyclic voltammograms of GCE/ZnO/RMs in blank aqueous acidic solution (pH 1.5). Two pairs of reversible redox peaks were observed at formal potentials $E_I^{0'}$ = +0.2 V and $E_{II}^{0'}$ = +0.36 V. These redox peaks (1 and 2) are ascribed to the redox reaction of electrogenerated tryptamine-4,5-dione (TAD) and 4,5-dihydroxytryptamine (DHT), respectively [40,42]. As shown in Fig. 2, the anodic and cathodic peak currents of peaks 1 and 2 were linearly dependent on scan rate with the linear equation of I_{pa1} and I_{pa2}, as shown in the inset of the figure, and the ratio of anodic peak current to cathodic peak current (I_{pa}/I_{pc}) was nearly equal to unity (see inset).

The separations of peak potentials (ΔE_p) for two redox peaks were 12 (peak 1) and 32 (peak 2) at a low scan rate (20 mV/s). For an ideal system, ΔE_p should be zero; however, this is not the usual case for most of the modified electrodes reported so far [44]. This nonzero ΔE_p may arise due to the interfacial salvation or slow electron transfer kinetics. With an increasing scan rate, ΔE_p would not be changed up to 200 mV/s (Fig. 2). The above results suggested that an electrochemical response of the GCE/ZnO/RMs is anticipated for a surface-confined redox process [45]. Therefore, the peak currents could be correlative with scan rate by the following equation [46]:

$$I_p = n^2F^2A\Gamma v/4RT \quad (4)$$

where Γ represents the surface coverage concentration (mol/cm^2), v is the scan rate, A (0.0707 cm^2) is the electrode surface area, and I_p is the peak current. The slopes of anodic peak current against scan rate for peaks 1 and 2 were −0.183 and −0.112 V, respectively. Thus, the calculated surface concentrations of peaks 1 and 2 were 2.5104×10^{-10} and 1.6719×10^{-10} mol/cm^2, respectively, further confirming the immobilized state of the RMs on the electrode surface.

The effect of pH value of the supporting electrolyte solution on the electrochemical response of GCE/ZnO/RM film-modified electrode was also investigated. With respect to the pH of the supporting electrolyte, both of the reversible redox peaks were shifted negatively (Fig. 3). The formal potentials ($E^{0'}$) linearly depended on pH value varying from 1 to 12 with slopes of −62 mV/pH (peak 1) and −60 mV/pH (peak 2), indicating that the total numbers of electrons and protons taking part in the charge transfer were the same (see inset of Fig. 3). Collectively, the electrode reactions of the GCE/ZnO/RMs are presented in Scheme 1 (Eqs. 5 and 6) [40,42,43].

SEM and AFM analysis

SEM images were taken on ZnO/RM film-coated ITO electrode, as shown in Fig. 4A. Core/Shell-like particles were observed, and the approximate size of the particles was found to be in the range of 1 to 2 μm. The inset of Fig. 4A shows the high magnification image of a single core/shell particle, and the particle size was approximately 2 μm. Fig. 4B shows the AFM image of ZnO/RM-coated electrode that corresponds to two-dimensional images and is recorded over an area of 20,000 × 20,000 nm. From AFM studies,

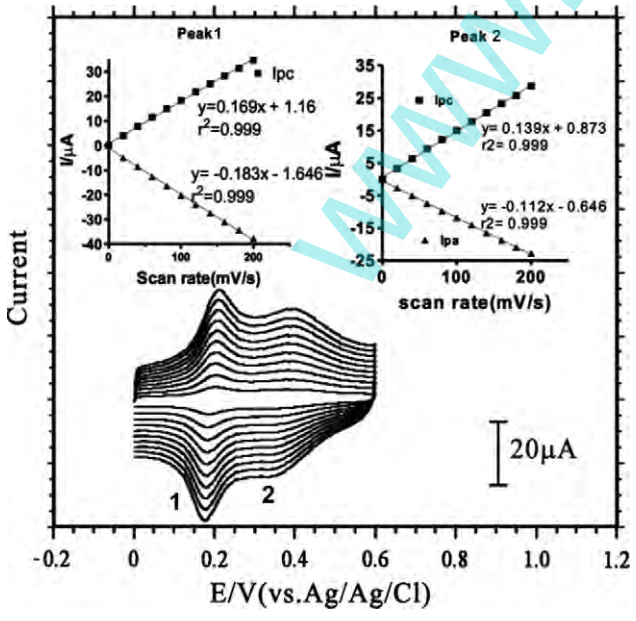

Fig. 2. Cyclic voltammograms of GCE/ZnO/RM-coated electrode in 0.1 M HNO_3 at different scan rates. The scan rates from inner to outer are 0.02, 0.04, 0.06, 0.08, 0.10, 0.12, 0.14, 0.16, 0.18, and 0.20 V/s. The inset shows the plot of I_{pa} and I_{pc} versus the scan rate for peaks 1 and 2.

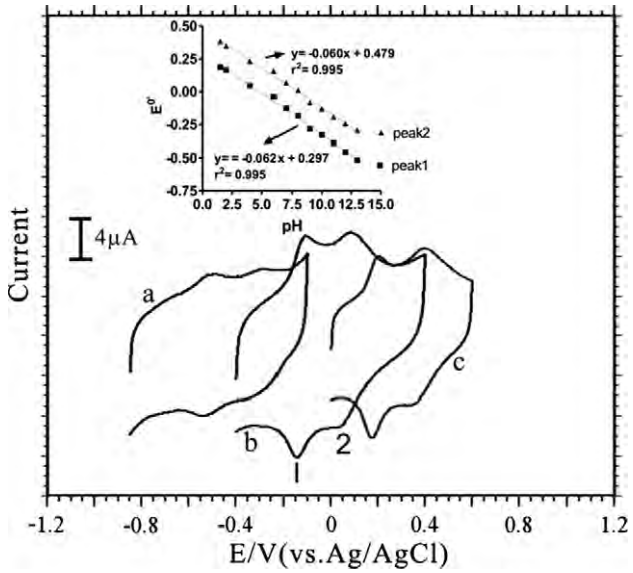

Fig. 3. Cyclic voltammograms of GCE/ZnO/RM-coated electrode in different pH values: (a) 12.0; (b) 7.0; (c) 1.5. Scan rate = 50 mV/s. The inset shows E^0as a function of pH for peaks 1 and 2.

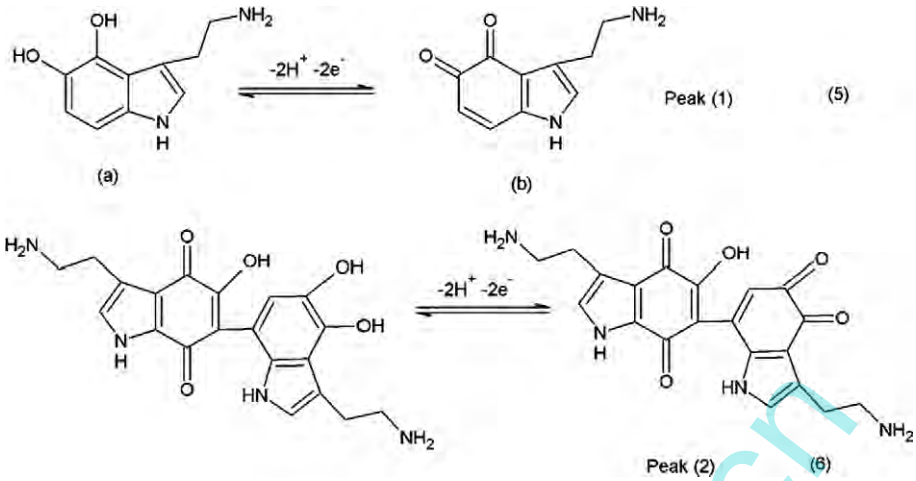

Scheme 1. Redox reactions of electrogenerated mediators.

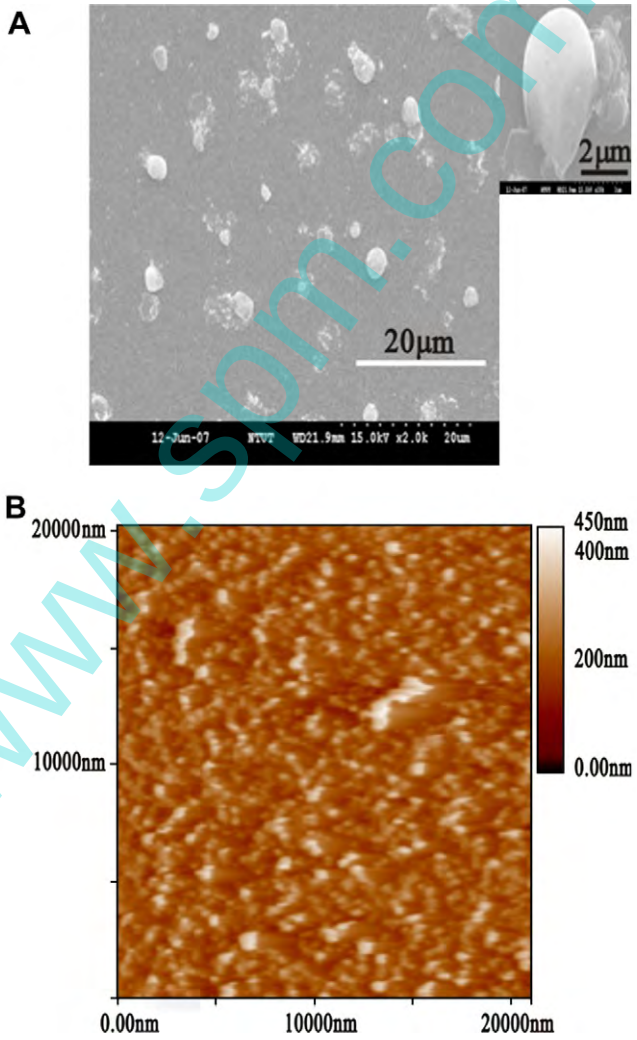

Fig. 4. SEM (A) and AFM (B) images of ZnO/RM-coated electrode. The inset in panel A shows a high-magnification image of single core/shell particle.

the ZnO/RM core/shell particle sizes were found to be in the range of 1 to 2 μm. The approximate film thickness of the ZnO/RMs was also found to be 450 ± 20 nm. When the AFM image was compared with the SEM image, the irregular surface coverage was seen more in the SEM image than in the AFM image because of the larger surface area used for SEM measurements (three times bigger than AFM scale). Based on SEM and AFM studies, we confirmed the ZnO/RM core/shell particles on the electrode surface.

Electrocatalytic oxidation of DA

Fig. 5 shows the cyclic voltammograms of 60 μM DA in phosphate-buffered saline (PBS, pH 7.0) at a GCE/ZnO and a GCE/ZnO/RMs. At a GCE/ZnO, an anodic peak was observed with an oxidation peak potential of 0.23 V, a reduction peak potential of 0.11 V (curve a′), and a peak separation (ΔE_p) of 120 mV. Under the same conditions, the GCE/ZnO/RMs gave highly enhanced redox peak currents and a more reversible electron transfer process to DA. A well-defined and stable redox wave of DA was observed, with anodic and cathodic peak potentials of 0.19 and 0.17 V, respectively (curve b). The separation of peak potentials (ΔE_p) at the GCE/ZnO/RMs was 20 mV, in accordance with Nernst reversible behavior, and identified that the number of electrons involved in the reaction was approximately 2. An intensive increase in DA peak current was also observed owing to the improvement in the reversibility of electron transfer process due to the larger real surface area of the GCE/ZnO/RMs. This suggests an efficient catalytic activity toward DA at the GCE/ZnO/RMs. The effect of scan rate on the anodic peak current (I_{pa}) of DA was studied by cyclic voltammetry (CV). With the scan rate increasing, the I_{pa} increased. Good linearity between the scan rate and I_{pa} was obtained within the range of 10 to 100 mV/s, suggesting a surface-confined process of DA on the modified electrode surface. The linear equation was I_{pa} (μA) = −0.18x − 1.63 (r^2 = 0.998). The effects of pH on the E_{pa} and peak currents were examined by CV in the presence of 50 μM DA in aqueous buffer solution with increasing pH from 2.0 to 10.0. The E_{pa} shifted negatively and was linearly dependent on pH, with the slope of −60 mV/pH indicating that the proportion of electrons and protons involved in the redox reaction of DA was 1:1 and that the oxidation of DA at GCE/ZnO/RM-modified electrode had been inferred to be a double electron transfer reaction. It could also be observed that both the oxidation and reduction peak currents obtained a maximum at pH 7.0. Although pH was below 7.0, the NH_2 group of quinone–imine structure could form NH_3^+ cations and exclude the DA positive ions. However, an increase in pH of the electrolyte above 7.0 decreased DA oxidation peak currents. Hence, pH 7.0 was chosen as the optimum pH for the electrocatalytic oxidation of DA at the GCE/ZnO/RMs.

It has been reported that positively charged mediators such as quinone–imine structure are efficient catalysts for electrocatalytic oxidation of NADH [47–49]. In the current investigation, we found that the quinone–imine structure of RMs can be useful for effective electrocatalytic oxidation of DA in neutral condition. According to the above discussion, the mechanism of DA oxidation at this modified electrode could be described as in Scheme 2. During oxidation of DA on RM film (DHT peak), DA undergoes a two-electron oxidation process resulting in dopamine-*o*-quinone (DOQ) (Eq. 7).

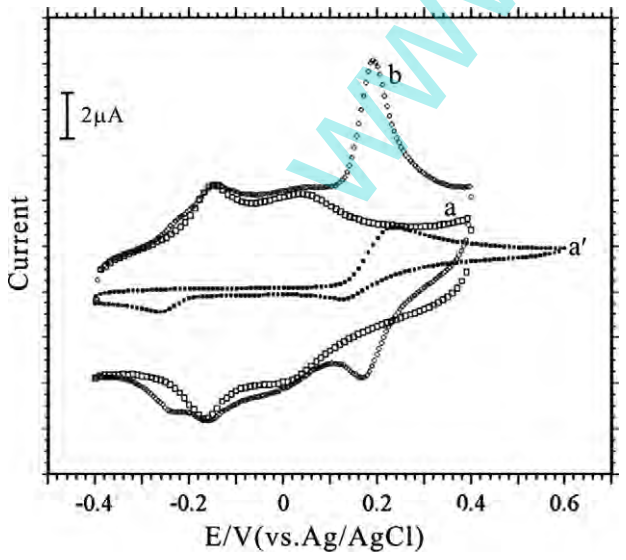

Fig. 5. Cyclic voltammograms of GCE/ZnO/RM-coated electrodes in 0.1 PBS (pH 7.0) containing DA = 0.0 μM (a); 60 μM (b); 60 μM with GCE/ZnO electrode (a′). Scan rate = 20 mV/s.

Effect of interferences on electrode response

AA and UA are the most important interferences in biological samples. Moreover, at bare electrodes, the oxidation of AA and UA occurred at a potential close to that of DA. Therefore, it is very important to measure the DA without interferences. To test these interferences, we analyzed the phosphate buffer solution (pH 7.0) in the presence of 60 μM DA, 150 μM AA, and 150 μM UA using GCE/ZnO/RM-coated electrode. Interestingly, as can be seen in Fig. 6 (curve b), three separate anodic oxidation peaks were identified with the well peak separation. The anodic oxidation potentials were 0.02, 0.184, and 0.31 V for AA, DA, and UA, respectively. The peak-to-peak separations between AA and DA and between DA and UA were 160 and 130 mV, respectively.

As can be readily seen in Fig. 6, the DHT redox peak efficiently mediates the oxidation of AA according to Scheme 2 (8). An enormous increase in the anodic peak current associated with a decrease in the cathodic peak was observed, demonstrating the strong electrocatalytic effect of the mediator. The oxidation potential of AA was 60 mV lower than the $E^{0'}$ of DHT redox peak, suggesting the highly efficient nature of the mediator. In this case, the electrogenerated redox mediator would be positively charged at the experimental condition used [40,42]. Because DHT is positively charged and has a quinone–imine structure, it showed an excellent catalytic effect toward AA.

ZnO/RM-modified electrode greatly enhanced the anodic peak currents of AA, DA, and UA. This dual behavior may arise due to the hydrophilic and hydrophobic nature of the RM film. It was established that poly(pyrrole) and poly(3,4-ethylenedioxythiophene) films have oxidized and reduced regions on their surface [50–53]. Reduced regions are hydrophobic and oxidized regions are hydrophilic in nature for the case of poly(3,4-ethylenedioxythiophene) [53]. The same behavior is expected for RM film, and this behavior may be responsible for simultaneous separation of AA and DA. Reduced regions on polymer surface may act as sites for oxidation of DA and UA molecules as described in Scheme 2 (Eqs. 7 and 9). As we expected, GCE/ZnO-coated electrode failed to do the same (curve c in Fig. 6). Based on this result, it may be possible to use GCE/ZnO/RM-coated electrode for simultaneous detection of AA, DA, and UA in neutral condition.

To ascertain the contribution of ZnO particles in this modified electrode, the electrocatalytic oxidation of 6 μM DA and 15 μM AA was examined using GCE/RM- and GCE/ZnO/RM-modified electrodes in PBS (Figs. 7AB). As expected, when compared with GCE/RMs, the catalytic current increased by 13 and 15% for AA and DA, respectively, on GCE/ZnO/RM-modified electrode, clearly indicating effective catalytic oxidation reactions of AA and DA on hybrid film-modified electrode. The increase in oxidation current in the presence of ZnO particles is attributed to the larger surface area and fast electron transfer kinetics of ZnO. Oxide particles are positively charged in neutral pH because of its high isoelectric point (9.5) [54,55], favoring weak adsorption of AA on ZnO particles. In addition, the reversibility of TAD and DHT redox systems is greatly enhanced on the surface of ZnO film because of its good semiconducting properties (Fig. 7). The larger surface area of ZnO particle-modified electrode may help the strong adsorption of oxidation products of SN, and its good semiconducting properties helped to achieve more reversibility and a higher number of active sites on

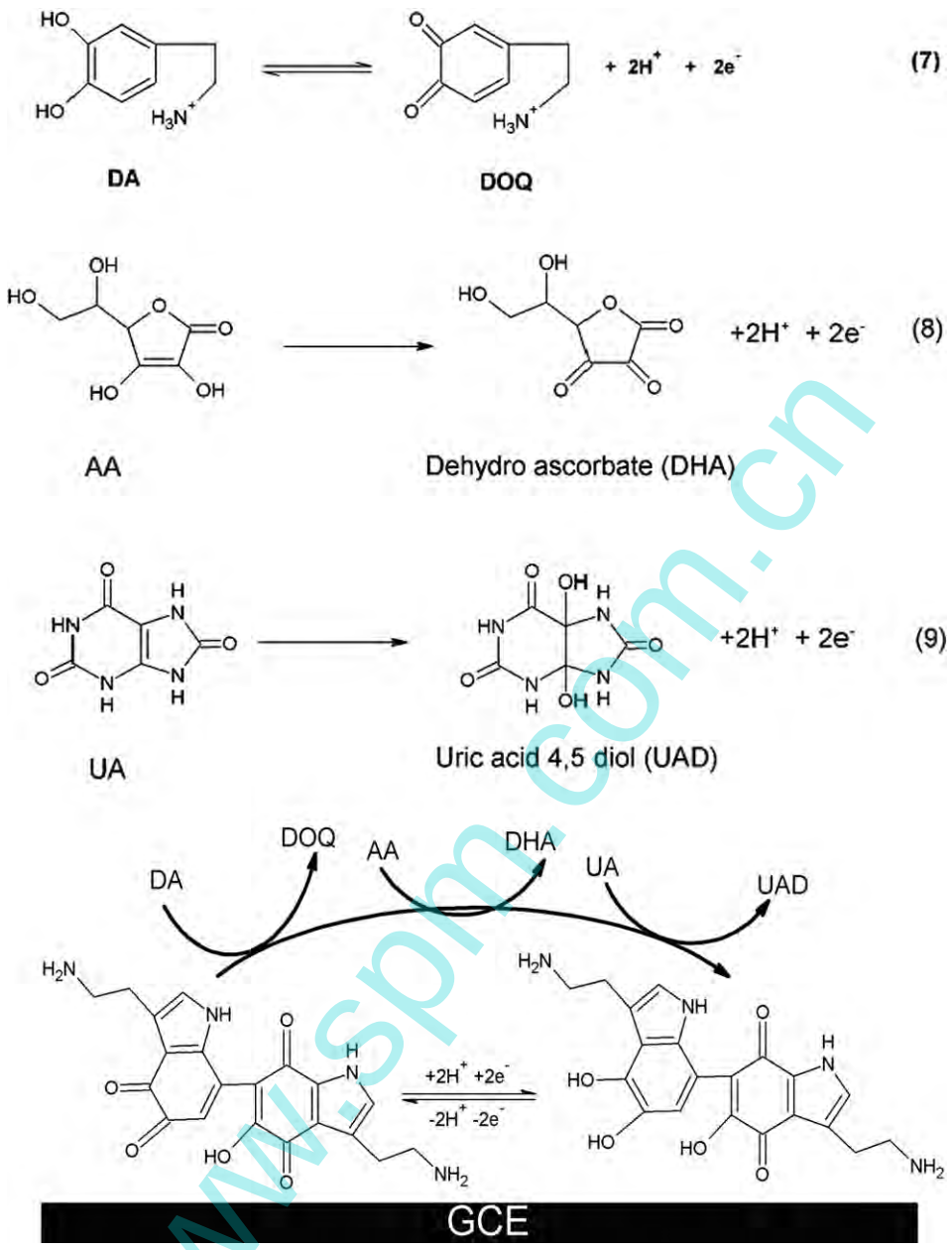

Scheme 2. Electrochemical oxidation reactions of DA, AA, and UA at ZnO/RM film-modified electrode.

the electrode surface, which results the higher catalytic currents for AA and DA. For these reasons, we prepared GCE/ZnO/RM hybrid film and used it for electroanalysis of AA, DA, and UA.

Simultaneous detection of DA, AA, and UA

The next attempt was taken to detect DA, AA, and UA simultaneously by using the GCE/ZnO/RM hybrid film-coated electrode. The CV results showed that the simultaneous determination of DA, AA, and UA could be possible at the GCE/ZnO/RM electrode. Under the optimized conditions, the CV curves of GCE/ZnO/RMs were obtained in 0.1 M PBS containing various concentrations of AA, DA, and UA, as shown in Fig. 8. The presence of ZnO/RM film on the GCE resolved the mixed voltammetric responses into three well-defined voltammetric peaks at potentials 20, 184, and 313 mV, corresponding to the oxidation of AA, DA, and UA, respectively. The separation among the three peak potentials is sufficient for the simultaneous determination of AA, DA, and UA. In addition, a substantial increase in peak currents was observed due to the improvements in the reversibility of the electron transfer processes. From the data obtained from Fig. 8, the calibration curves for AA, DA, and UA were linear for the whole concentration range investigated (1.5×10^{-5} to 2.4×10^{-4} M for AA, 6×10^{-6} to 9.6×10^{-4} M for DA, and 5×10^{-5} to 8×10^{-4} M for UA) with the correlation coefficients 0.991, 0.992, and 0.989, respectively.

To investigate the degree of interferences on the peak current of DA, cyclic voltammograms were recorded in 0.1 M PBS containing 60 μM DA in the absence of 150 μM AA (curve a in Fig. 9) and the presence of 150 μM AA (curve b in Fig. 9). In the presence of AA, the anodic peak current of DA was increased approximately 6% without a distinct change in oxidation potential. For the case of UA, the DA peak current was increased up to 3%. As can be seen in Fig. 9, three independent oxidation waves emerged for AA, DA, and UA at ZnO/RM-coated electrode. Based on our experimental results, the partial overlapping of AA with DA oxidation peak is insignificant for determination of DA.

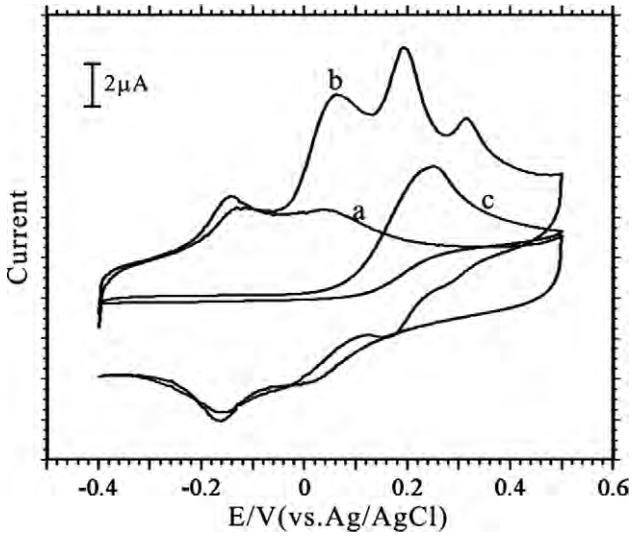

Fig. 6. Cyclic voltammograms were recorded in PBS (pH 7.0) using GCE/ZnO/RM electrode in 0.0 μM (a); 60 μM DA, 150 μM AA, and 150 μM UA (b); and GCE/ZnO-coated electrode with 60 μM DA, 150 μM AA, and 150 μM UA (c).

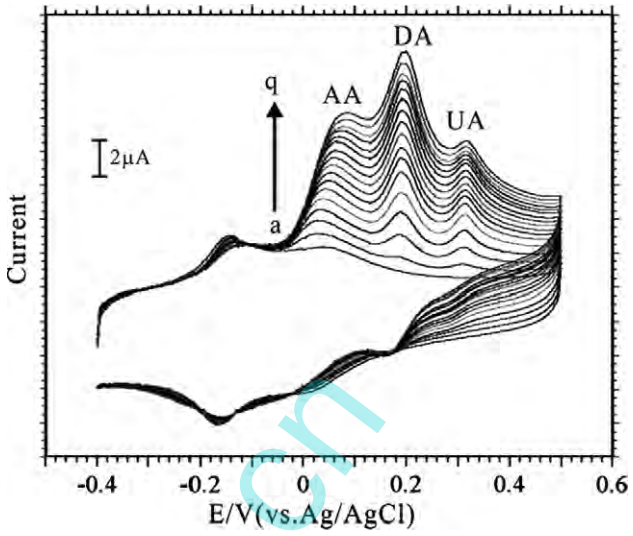

Fig. 8. Cyclic voltammograms of GCE/ZnO/RMs in PBS (pH 7.0) containing different concentrations of AA, DA, and UA: (a) 0.0 μM; (b–q) each addition increased 6 μM DA, 15 μM AA, and 50 μM UA.

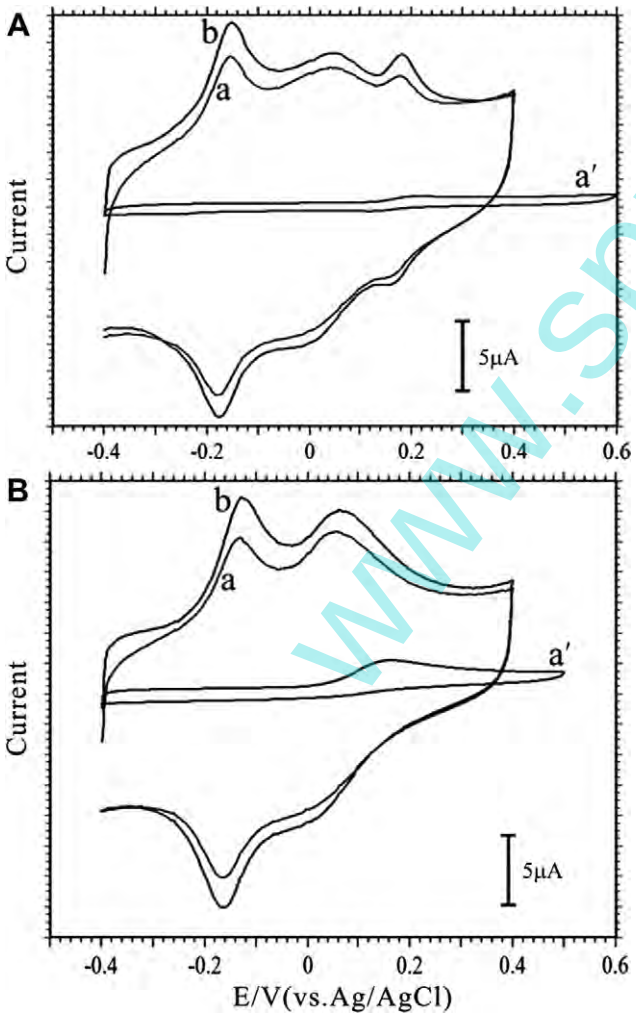

Fig. 7. Cyclic voltammograms were recorded using GCE/RMs (curve a) and GCE/ZnO/RMs (curve b) in 0.1 M PBS containing 6 μM DA (A) and 15 μM AA (B). Curve a′ was obtained for both DA and AA using GCE/ZnO-coated electrode. Scan rate = 50 mV/s.

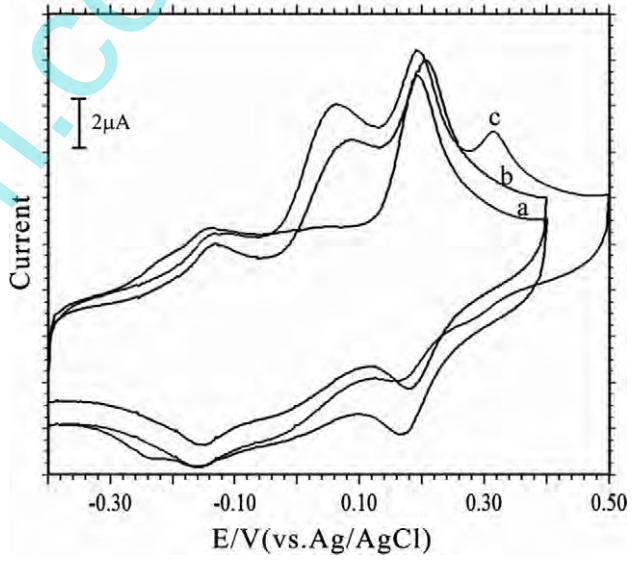

Fig. 9. Cyclic voltammograms were recorded using GCE/ZnO/RMs in 0.1 M PBS containing 60 μM DA (curve a), 60 μM DA + 150 μM AA (curve b), and 60 μM DA + 150 μM AA + 500 μM UA (curve c).

Amperometric determination of DA

The amperometric response of the GCE/ZnO/RMs for the measurements of DA was examined. The amperograms were obtained in a series of concentrations of DA at fixed 0.25 V, and the obtained results are shown in Fig. 10. On the addition of 6 μM DA, the GCE/ZnO/RMs respond favorably to each of the additions, yielding steady-state signals within 5 s. These data indicate that this new modified electrode has higher electrocatalytic activity toward DA oxidation. A calibration curve of current (I) versus concentrations (c) for DA was obtained at this modified electrode. The dependence of current response on the concentration of DA was linear in the range from 6×10^{-6} to 1.2×10^{-4} M (see inset of Fig. 10); after this linear range, the current signal starts to show signs of saturation. The calibration curve was obtained with the linear regression

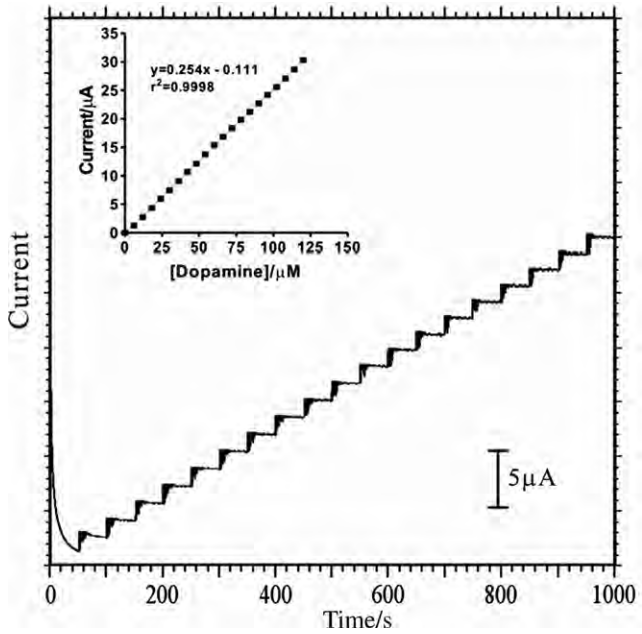

Fig. 10. Amperograms of GCE/ZnO/RMs in PBS (pH 7.0) with increasing DA concentrations in the range from 6 to 120 μM. Applied potential = 0.25 V The inset shows I_{pa} versus DA concentrations.

equation of I_{pa} (μA) = 0.254x – 0.111 with a good correlation coefficient of r = 0.9998. The detection limit (signal/noise = 3) was estimated to be 0.5 μM. This amperometric method is not useful for the detection of DA in real samples in the presence of AA. But from the experimental data, one can see that reproducible and stable analytical signals can be obtained for determination of DA at GCE/ZnO/RM hybrid film-coated electrode (Fig. 10).

The pH used, linear range, and detection limit of various electroanalytic methods proposed for simultaneous determination of AA, DA, and UA are compared with our analytical data in Table 1. From the data shown, a lower limit of detection (LOD) [23,32,34,35] and wide linear range for the detection of AA can be achieved using the proposed method. A lower LOD [23,34] and wide linear range for the detection of DA is possible using ZnO/RM hybrid film-coated electrode [23,32,33,35,36]. A lower LOD [34,36] and wide linear range for UA detection is demonstrated using our proposed method [23,32–36]. Our results are good comparable with existing methods for the detection of AA, DA, and UA, and this new method can be useful for electroanalysis of AA, DA, and UA.

Electroanalysis of real samples

We tested the real applicability of ZnO/RM hybrid film-coated electrode for the determination of AA in commercially available vitamin C tablets, DA in dopamine hydrochloride injection, and UA in spiked samples. An accurately weighed vitamin C tablet was finely powdered, and 100 mg of tablet powder was dissolved in 25 ml of distilled water and ultrasonicated for 5 min to make homogeneous solution. 1 ml of AA tablet solution was mixed with 9 ml of 0.1 M PBS and used for investigation by CV. The obtained results are presented in Table 2. DA injection was diluted with doubly distilled water, and then a portion of diluted solution was mixed with 0.1 M PBS and analyzed using ZnO/RM hybrid film-coated electrode in CV (Table 3). To test the degree of interference on the analytical signal of UA, the known amount of UA solution was spiked in DA injection solution. Thereafter, the spiked sample was analyzed in 10 ml of 0.1 M PBS using the proposed method. In

Table 1
Comparison of electroanalytic methods proposed for determination of AA, DA, UA

Modified electrode	pH used	[Ascorbic acid]		[Dopamine]		[Uric acid]		Reference
		Linear range(μM)	Detection limit(μM)	Linear range(μM)	Detection limit(μM)	Linear range(μM)	Detection limit(μM)	
Poly(vinyl alcohol) covalently modified GCE	7.0	10–250	7.6	2–70	1.4	2–50	0.6	[23]
Poly(eriochrome black T)/GCE	4.0	150–1000	10	0.1–200	0.02	10–130	1.0	[32]
Poly(acrylic acid)-multiwalled carbon nanotube composite-covered GCE	7.4	–	–	0.04–3	20 nM	0.3–10	110 nM	[33]
PtAu hybrid film-modified GCE	4.0	24–384	24	103–1650	103	21–336	21	[34]
DA-modified PGE	10.0	25–500	13	1–20	0.11	2.5–20	1.4	[35]
Sol–gel carbon ceramic composite electrode	5.0	0.5–20	0.1	0.5–20	0.1	10–200	5	[36]
ZnO/RMs hybrid film-coated GCE	7.0	15–240	1.4	6–960	0.7	50–800	4.5	This work

Table 2
Results for the determination of AA in commercial tablets

Vitamin C tablet sample	Labeled value(mg)	Proposed method[a](mg)	RSD(%)	Recovery(%)
A	500	497.28	2.93	99.46
B	500	501.82	2.57	100.36
C	500	503.18	1.86	100.64

[a] Each value is an average of three replicate determinations.

Table 3
Determination of DA in injection

Tested sample	Added (μg/ml)	Found[a] (μg/ml)	RSD (%)	Recovery (%)
A	40	39.14	3.42	97.85
B	40	40.57	2.46	101.43
C	40	40.83	2.18	102.08

[a] Each value is an average of three replicate determinations.

Table 4
Determination of UA in spiked samples

Tested sample	Added (μg/ml)	Found[a] (μg/ml)	RSD (%)	Recovery (%)
A	40	39.14	3.42	97.85
B	40	40.57	2.46	101.43
C	40	40.83	2.18	102.08

[a] Each value is an average of three replicate determinations.

real-sample experiments, the concentration of unknowns was calculated using the standard addition method. The obtained analytical data are given in Table 4. From the real-sample analysis, the precision and reliability of the proposed method are good. In addition, the recovery ratio on the basis of this method was investigated, and the values are provided in Tables 2 to 4. The recovered ratio indicates that the determination of AA, DA, and UA using the ZnO/RM hybrid film-coated electrode is effective and can be applied for their detection in real samples.

Stability and reproducibility of ZnO/RM-coated electrode

The stability of the GCE/ZnO/RM-coated electrode was investigated by measuring the current responses to 100 μM DA after every few days stored at 5 °C in PBS (pH 7.0). After 6 weeks, the response currents of the ZnO/RM-coated electrode decreased gradually to 85% of the initial values. The relative standard deviation (RSD) of nine measurements of 100 μM DA with the same GCE/ZnO/RM-coated electrode was 3.6%. Furthermore, the stability of GCE/ZnO/RM electrode was examined by successive potential cycling between –0.4 and 0.4 V at a scan rate of 0.1 V s^{-1}. Under continuous potential sweeping, an insignificant decay in the peak currents was observed during the initial cycles (2% for first 50 cycles), and the rate of current decrease then decreased (5% after 600 cycles). It can be observed that the electrode current remained stable on continuous cycling of even more than 600 cycles. Also, the electrode was found to be reproducible after the DA oxidation, indicating that surface fouling was not observed with the modified electrode. These results suggested that GCE/ZnO/RMs have long-term stability and that reproducible analytical signal can be obtained. In addition, the proposed modified electrode can be prepared within 30 min, so it can be prepared easily.

Conclusions

We have reported a new modified electrode, GCE/ZnO/RMs, for simultaneous detection of AA, DA, and UA. SEM and AFM images of ZnO/RM film revealed that core/shell-like particles were obtained and that the surfaces are well microstructured. The GCE/ZnO/RM electrode acted as a sensor and displayed good electrocatalytic activity toward AA, DA, and UA. The GCE/ZnO/RM electrode used for simultaneous measurements of AA, DA, and UA were in the ranges from 1.5×10^{-5} to 2.4×10^{-4} M, 6×10^{-6} to 9.6×10^{-4} M, and 5×10^{-5} to 8×10^{-4} M, respectively. This is a very simple method for electrode fabrication and can be very useful for detection of DA, AA, and UA in physiological solution.

Acknowledgment

This work was supported financially by the Ministry of Education and the National Science Council of Taiwan, Republic of China.

References

[1] L. Schmidt-Mende, J.L. MacManus-Driscoll, ZnO: Nanostructures, defects, and devices, Mater. Today 10 (2007) 40–48.
[2] M.C. Newton, P.A. Warburton, ZnO tetrapod nanocrystals, Mater. Today 10 (2007) 50–54.
[3] P.X. Gao, C.S. Lao, Y. Ding, Z.L. Wang, Metal/Semiconductor core/shell nanodisks and nanotubes, Adv. Funct. Mater. 16 (2006) 53–62.
[4] S. Karuppuchamy, K. Nonomura, T. Yoshida, T. Sugiura, H. Minoura, Cathodic electrodeposition of oxide semiconductor thin films and their application to dye-sensitized solar cells, Solid State Ionics 151 (2002) 19–27.
[5] J.X. Wang, X.W. Sun, A. Wei, Y. Lei, X.P. Cai, C.M. Li, Z.L. Dong, Zinc oxide nanocomb biosensor for glucose detection, Appl. Phys. Lett. 88 (2006) 233106.
[6] M.H. Huang, S. Mao, H. Feick, H.Q. Yan, Y.Y. Wu, H. Kind, E. Weber, R. Russo, P.D. Yang, Room-temperature ultraviolet nanowire nanolasers, Science 292 (2001) 1897–1899.
[7] Z.W. Pan, Z. Dai, Z.L. Wang, Nanobelts of semiconducting oxides, Science 291 (2001) 1947–1949.
[8] Y. Dai, Y. Zhang, Q.K. Li, C.W. Nan, Synthesis and optical properties of tetrapod-like zinc oxide nanorods, Chem. Phys. Lett. 358 (2002) 83–86.
[9] Y.J. Xing, Z.H. Xi, X.D. Zhang, J.H. Song, R.M. Wang, J. Xu, Z.Q. Xue, D.P. Yu, Nanotubular structures of zinc oxide, Solid State Commun. 129 (2004) 671–675.
[10] X.Y. Kong, Z.L. Wang, Polar-surface dominated ZnO nanobelts, the electrostatic energy induced nanohelixes, nanosprings, and nanospirals, Appl. Phys. Lett. 84 (2004) 975–977.
[11] X.Y. Kong, Y. Ding, R. Yang, Z.L. Wang, Single-crystal nanorings formed by epitaxial self-coiling of polar nanobelts, Science 303 (2004) 1348–1351.
[12] A. Walcarius, Electrochemical applications of silica-based organic–inorganic hybrid materials, Chem. Mater. 13 (2001) 3351–3372.
[13] R. Gangopadhyay, A. De, Conducting polymer nanocomposites: A brief overview, Chem. Mater. 12 (2000) 608–622.
[14] J. Macanás, M. Farre, M. Muñoz, S. Alegret, D.N. Muraviev, Preparation and characterization of polymer-stabilized metal nanoparticles for sensor applications, Phys. Stat. Sol. 203 (2006) 1194–1200.
[15] P. Damier, E.C. Hirsch, Y. Agid, A.M. Graybiel, The substantia nigra of the human brain: II. Patterns of loss of dopamine-containing neurons in Parkinson's disease, Brain 122 (1999) 1437–1448.
[16] C. Martin, The Parkinson's puzzle: New developments in our understanding of Parkinson's disease have generated a number of promising new treatments for this disabling condition, Chem. Br. 34 (1998) 40–42.
[17] R.M. Wightman, L.J. May, A.C. Michael, Detection of dopamine dynamics in the brain, Anal. Chem. 60 (1988) 769A–779A.
[18] A. Heinz, H. Przuntek, G. Winterer, A. Pietzcker, Clinical aspects and follow-up of dopamine-induced psychoses in continuous dopaminergic therapy and their implications for the dopamine hypothesis of schizophrenic symptoms, Nervenarzt 66 (1995) 662–669.
[19] R.D. O'Neill, Microvoltammetric techniques and sensors for monitoring neurochemical dynamics in vivo: A review, Analyst 119 (1994) 767–779.
[20] A. Ciszewski, G. Milczarek, Polyeugenol-modified platinum electrode for selective detection of dopamine in the presence of ascorbic acid, Anal. Chem. 71 (1999) 1055–1061.
[21] V.S.E. Dutt, H.A. Mottola, Determination of uric acid at the microgram level by a kinetic procedure based on a pseudo-induction period, Anal. Chem. 46 (1974) 1777–1781.

[22] G.G. Guilbgault, Analytical Uses of Immobilized Enzymes, Marcel Dekker, New York, 1984.
[23] Y.X. Li, X.Q. Lin, Simultaneous electroanalysis of dopamine, ascorbic acid, and uric acid by poly(vinyl alcohol) covalently modified glassy carbon electrode, Sens. Actuat. B 115 (2006) 134–139.
[24] G.Y. Jin, Y.Z. Zhang, W.X. Cheng, Poly(*p* -aminobenzene sulfonic acid)-modified glassy carbon electrode for simultaneous detection of dopamine and ascorbic acid, Sens. Actuat. B 107 (2005) 528–534.
[25] H.T. Xu, F. Kitamura, T. Ohsaka, K. Tokuda, Simultaneous determination of dopamine and ascorbic acid with poly(3-methylthiophene)/polypyrrole bilayer-coated carbon fiber electrodes, Anal. Sci. 10 (1994) 399–404.
[26] G. Erdogdu, H.B. Mark Jr., E. Karagozler, Voltammetric resolution of ascorbic acid and dopamine at conducting polymer electrodes, Anal. Lett. 29 (1996) 221–231.
[27] W. Chen, X.H. Lin, L.Y. Huang, H.B. Luo, Electrochemical characterization of polymerized cresol red film modified glassy carbon electrode and separation of electrocatalytic responses for ascorbic acid and dopamine oxidation, Microchim. Acta 151 (2005) 101–107.
[28] W. Chen, X.H. Lin, L.Y. Huang, H.B. Luo, Electrocatalytic behavior and voltammetric determination of dopamine on a poly(bromophenol blue) modified electrode, Chin. J. Anal. Lab. 5 (2005) 8–11.
[29] X. Lin, Q. Zhuang, J. Chen, S. Zhang, Y. Zheng, Electrocatalytic property of poly-chromotrope 2B modified glassy carbon electrode on dopamine and its application, Sens. Actuat. B 125 (2007) 240–245.
[30] P. Shakkthivel, S.M. Chen, Simultaneous determination of ascorbic acid and dopamine in the presence of uric acid on ruthenium oxide modified electrode, Biosens. Bioelectron. 22 (2007) 1680–1687.
[31] S.A. Kumar, C.F. Tang, S.M. Chen, Poly(4-amino-1-1′-azobenzene-3,4′-disulfonic acid) coated electrode for selective detection of dopamine from its interferences, Talanta 74 (2008) 860–866.
[32] H. Yao, Y. Sun, X. Lin, Y. Tang, L. Huang, Electrochemical characterization of poly(eriochrome black T) modified glassy carbon electrode and its application to simultaneous determination of dopamine, ascorbic acid, and uric acid, Electrochim. Acta 52 (2007) 6165–6171.
[33] A. Liu, I. Honma, H. Zhou, Simultaneous voltammetric detection of dopamine and uric acid at their physiological level in the presence of ascorbic acid using poly(acrylic acid)-multiwalled carbon-nanotube composite-covered glassy-carbon electrode, Biosens. Bioelectron. 23 (2007) 74–80.
[34] S. Thiagarajan, S-M. Chen, Preparation and characterization of PtAu hybrid film modified electrodes and their use in simultaneous determination of dopamine, ascorbic acid, and uric acid, Talanta 74 (2007) 212–222.
[35] R.P. da Silva, A.W.O. Lima, S.H.P. Serrano, Simultaneous voltammetric detection of ascorbic acid, dopamine, and uric acid using a pyrolytic graphite electrode modified into dopamine solution, Anal. Chim. Acta 612 (2008) 89–98.
[36] A. Salimi, H. MamKhezri, R. Hallaj, Simultaneous determination of ascorbic acid, uric acid, and neurotransmitters with a carbon ceramic electrode prepared by sol–gel technique, Talanta 70 (2006) 823–832.
[37] S.A. Kumar, S.M. Chen, Fabrication and characterization of Meldola's blue/zinc oxide hybrid electrodes for efficient detection of the reduced form of nicotinamide adenine dinucleotide at low potential, Anal. Chim. Acta 592 (2007) 36–44.
[38] S.A. Kumar, S.M. Chen, Electrochemical, microscopic, and EQCM studies of cathodic electrodeposition of ZnO/FAD and anodic polymerization of FAD films modified electrodes and their electrocatalytic properties, J. Solid State Electrochem. 11 (2007) 993–1006.
[39] S.A. Kumar, S-M. Chen, Electrocatalysis and amperometric detection of the reduced form of nicotinamide adenine dinucleotide at toluidine blue/zinc oxide coated electrodes, Electroanalysis 19 (2007) 1952–1958.
[40] M.Z. Wrona, G. Dryhurst, Electrochemical oxidation of 5-hydroxytryptamine in aqueous solution at physiological pH, Bioorg. Chem. 18 (1990) 237–291.
[41] Y.N. Ivanova, A.A. Karyakin, Electropolymerization of flavins and the properties of the resulting electroactive films, Electrochem. Commun. 6 (2004) 120–125.
[42] M.Z. Wrona, G. Dryhurst, Oxidation chemistry of 5-hydroxytryptamine: I. Mechanism and products formed at micromolar concentrations, J. Org. Chem. 52 (1987) 2817–2825.
[43] B. Hoyer, N. Jensen, Stabilization of the voltammetric serotonin signal by surfactants, Electrochem. Commun. 8 (2006) 323–328.
[44] R.W. Murray, Chemically modified electrodes, in: A.J. Bard (Ed.), Electroanalytical Chemistry, vol. 13, Marcel Dekker, New York, 1984, pp. 191–368.
[45] A.P. Brown, F.C. Anson, Cyclic and differential pulse voltammetric behavior of reactants confined to the electrode surface, Anal. Chem. 49 (1977) 1589–1595.
[46] M. Sharp, M. Petersson, K. Edstrom, Preliminary determinations of electron transfer kinetics involving ferrocene covalently attached to a platinum surface, J. Electroanal. Chem. 95 (1979) 123–130.
[47] L. Gorton, E. Dominguez, Electrochemistry of NAD(P)t$^+$/NAD(P)H, in: G.S. Wilson (Ed.), Encyclopedia of Electrochemistry, vol. 9, Wiley–VCH, Weinheim Germany, 2002, pp. 67–143.
[48] S.M. Chen, M.I. Liu, S.A. Kumar, Electrochemical preparation of poly(acriflavine) film-modified electrode and its electrocatalytic properties towards NADH, nitrite, and sulfur oxoanions, Electroanalysis 19 (2007) 999–1007.
[49] C.R. Raj, S. Chakraborty, Carbon nanotubes–polymer–redox mediator hybrid thin film for electrocatalytic sensing, Biosens. Bioelectron. 22 (2006) 700–706.
[50] C.R. Martin, L.S. Van Dyke, Mass and charge transport in electronically conductive polymers, in: R.W. Murray (Ed.), Molecular Design of Electrode Surfaces, John Wiley, New York, 1992, pp. 403–424.
[51] M.E.G. Lyons, Charge percolation in electroactive polymers, in: M.E.G. Lyons (Ed.), Electroactive Polymer Electrochemistry, part 1, Plenum, New York, 1994, pp. 65–116.
[52] G. Schopf, G. Koßmehl, Polythiophenes: Electrically Conductive Polymers, Springer, Germany, 1997.
[53] S.S. Kumar, J. Mathiyarasu, K.L. Phani, Exploration of synergism between a polymer matrix and gold nanoparticles for selective determination of dopamine, J. Electroanal. Chem. 578 (2005) 95–103.
[54] F.F. Zhang, X.L. Wang, S.Y. Ai, Z.D. Sun, Q. Wan, Z.Q. Zhu, Y.Z. Xian, L.T. Jin, K. Yamamoto, Immobilization of uricase on ZnO nanorods for a reagentless uric acid biosensor, Anal. Chim. Acta 519 (2004) 155–160.
[55] Z. Liu, Y. Liu, H. Yang, Y. Yang, G. Shen, R. Yu, A mediator-free tyrosinase biosensor based on ZnO sol–gel matrix, Electroanalysis 17 (2005) 1065–1070.